Unusual trinuclear complex of copper(II) containing a 4'-(3-methyl-2-thienyl)-4,2':6',4 -terpyridine ligand. Structural, spectroscopic, electrochemical and magnetic properties

D. Toledo, G. Ahumada, C. Manzur, T. Roisnel, O. Peña, J.-R. Hamon, J.-Y. Pivan, Y. Moreno

Graphical Abstract

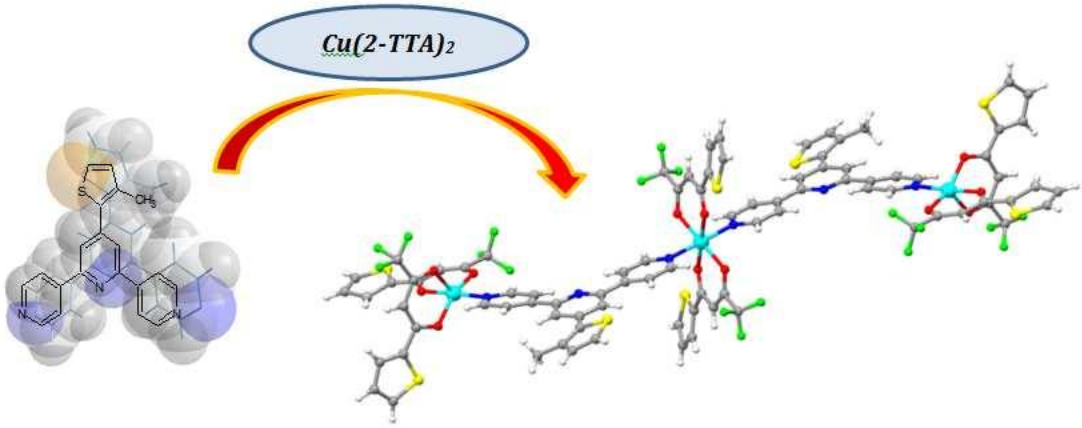

A trinuclear Cu(II) complex containing 4'-substituted-4,2':6',4''-terpyridine ligand, has been synthesized and structurally characterized by X-ray crystallography. Their spectroscopic, electrochemical and magnetic behavior has been established.

Unusual trinuclear complex of copper (II) containing a 4'-(3-methyl-2-thienyl)-4,2':6',4''-terpyridine ligand. Structural, spectroscopic, electrochemical and magnetic properties.

Dominique Toledo[a], Guillermo Ahumada[b,c], Carolina Manzur[b], Thierry Roisnel[c], Octavio Peña[c], Jean-René Hamon[c], Jean-Yves Pivan[c,d], Yanko Moreno[e*]

[a]Universidad de Concepción, Facultad de Ciencias Químicas, Departamento de Química Analítica e Inorgánica, Edmundo Larenas 129, Concepción, Chile.

[b] Laboratorio de Química Inorgánica, Instituto de Química, Pontificia Universidad Católica de Valparaíso, Campus Curauma, Avenida Universidad 330, Valparaíso, Chile.

[c] Institut des Sciences Chimiques de Rennes, UMR 6226 CNRS Université de Rennes 1, Campus de Beaulieu, 35042 Rennes cedex, France

[d] École Nationale Supérieure de Chimie de Rennes, UMR 6226 CNRS, 11 allée de Beaulieu, 35708 Rennes cedex 07, France

[e] Universidad Andrés Bello, Departamento de Ciencias Químicas, Facultad de Ciencias Exactas, C.P. 2520000, Viña del Mar, Chile.

Corresponding authors. Phone: +56 32 *284 59 62*, E-mail address: yanko.moreno@unab.cl (Y. Moreno).

ABSTRACT

We report the synthesis, characterization, crystal and molecular structure as well as the spectroscopic, electrochemical and magnetic properties of an unexpected trinuclear copper (II) complex **(1)**, made of three Cu(**2-TTA**)$_2$ units (**2-TTA** = 2-thenoyltrifluoroacetone) bridged by two 4'-(3-methyl-2-thienyl)-4,2':6',4''-terpyridine **(4-stpy)** ligands. The central Cu(II) atom shows an octahedral geometry, while the lateral metal centers present a slightly distorted square pyramidal coordination sphere. It is suggested that the introduction of the relatively bulky substituent groups (2-thienyl and –CF_3) in the **2-TTA** ligand are responsible of this uncommon coordination mode. The magnetic behavior of **1** is reported in terms of a combination of monomer and dimer units, leading to weak antiferromagnetic interaction (J= -1.93 cm^{-1}). The cyclovoltammogram of **1** exhibits, in the cathodic potential region, three redox events due to Cu^{2+}/Cu^{+} and Cu^{+}/Cu^{0} redox couples and to the mono-electronic reduction of the **4-stpy** ligand.

Keywords: Copper(II) complex; 4,2':6',4''-terpyridine; 2-thenoyltrifluoroacetonate; magnetic properties; cyclic voltammetry; crystal structure.

1. Introduction

The rational design and synthesis of Cu(II) complexes has been an interesting subject in the early development of supramolecular and metallosupramolecular chemistry. Due to their versatile structures, properties and reactivity, wide applications are found, such as: molecular magnetism [1-4] , catalysis [5,6] , biological activity [7-10], electrochemistry [11], etc. In these molecular materials, control of the coordination mode and the chemical reactivity of the metal ion can be assessed by a correct choice of the appropriate building blocks [12-14]. Within the vast family of divergent polypyridine ligands, the 4'-(substituted)-4,2':6',4"-terpyridines are of special interest because they are easily synthesized by an aldol condensation with a wide range of additional functionalities [15-17]. Their divergent arrangements of N-donor atoms and the incorporation of aryl substituents into the 4'-position of 4,2':6',4"-terpyridine allow to bridge two or more metal centers, giving rise, in the vast majority of cases, to metal-organic architectures of high stability, featuring mainly coordination polymers and frameworks [18-23].

In the search for stable molecular systems containing more than one paramagnetic metal center, in particular Cu(II), the bis(β-diketonate)metal(II) systems with planar structure have shown the ability to coordinate terpyridine derivatives, and this plays an important role in the structure, dimensionality and properties of the resulting compounds [24-27]. In particular, using bis(β-diketonate)metal(II) it is possible to adjust the acidity of the metal ion by varying the substituents of the starting β-diketones. For example, the electron withdrawing group of the β-diketonate ligand, such as $-CF_3$, increases the positive charge on the metal center, improving their ability to coordinate weak Lewis bases. On the other hand, various metal ions can be used to trigger different physical properties of the final systems [26-28]. Thereby, pursuing our recent work on some 4,2':6',4"-terpyridine derivatives, we now focus our efforts on the study of the ligand 4'-(3-methyl-2-thienyl)-4,2':6',4"-terpyridine (**4-stpy**) (**Scheme 1**) as complexing agent [29] in the copper(II) coordination chemistry. Herein, we report a successful attempt of the synthesis and structural exploration of the novel trinuclear complex, [Cu_3(**2-TTA**)$_6$(**4-stpy**)$_2$] **(1)** (**Scheme 2**), using **4-stpy** ligand and Cu(**2-TTA**)$_2$ (**2-TTA** = 2-thenoyltrifluoroacetonato ligand). Complex **1** has been fully characterized by classical spectroscopic methods. The electrochemical behavior has been studied, since the formation of a complex with a discrete structure and the presence of 2-thienyl units, opens up opportunities to the formation of polymeric [30,31] and metallopolymeric

materials [32,33], either through chemical or electrochemical oxidation of the thiophene units [34,35]. Moreover, thermal stabilities and magnetic properties of **1** are systematically discussed.

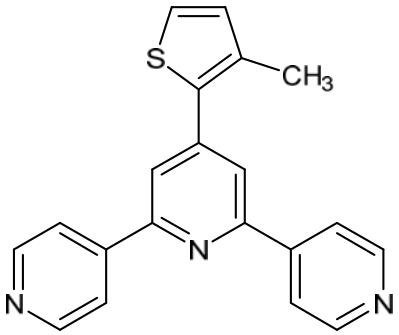

Scheme 1. Schematic description of **4-stpy**.

2. Experimental

2.1. General Experimental Methods

The **4-stpy** ligand and the Cu(**2-TTA**)$_2$ were prepared according to the literature [29,36]. All other chemicals were used as obtained from commercial sources without further purification. Solvents were dried and distilled under nitrogen by standard methods prior to use [37]. FT-IR spectra were recorded from KBr disks on a Perkin Elmer model 1600 FT-IR spectrophotometer, in the 4000-400 cm^{-1} range. UV-Vis absorption spectra of **4-stpy** and compound **1** were recorded in CH_2Cl_2 with a Shimadzu UV-1800 spectrophotometer. Thermogravimetric analysis was carried out with a Universal V2.6 DTA instrument under nitrogen atmosphere with a heating rate of 10 °C/min. The magnetic susceptibility was recorded between 2 K and 300 K, using a SQUID magnetometer (MPMS-XL) at an applied field of 500 Oe (0.05 Tesla). Powder samples were placed inside a gelatine capsule. The EPR spectrum was recorded on powder samples at room temperature with a BRUKER EMX spectrophotometer at an excitation frequency of 9.478305 GHz. Cyclic voltammetry (CV) measurements were performed using a CHI604E potentiostat and a standard three-electrode set-up (purged with argon and maintained under inert atmosphere) at 100 mV/s scan rate using a platinum working electrode, SCE reference and platinum wire auxiliary electrode, with a voltage scan rate of 100 mVs^{-1}. The concentration of compounds under investigation was 10^{-3} M in acetonitrile solution containing 0.1 M *n*-$Bu_4N^+PF_6^-$ as supporting electrolyte. Ferrocene (Fc) was added as an internal standard at the end of each

experiment. The Fc/Fc^+ couple was located at $E_{½}$ 0.40 V (ΔEp = 0.09 V; i_{pa}/i_{pc} = 1.0) [38], where $E_{½}$ was calculated from the average of the oxidation and reduction peak potentials. Microanalyses were conducted on a Thermo-FINNIGAN Flash EA 1112 CHNS/O analyzer implanted in the Microanalytical Service of the CRMPO at the University of Rennes 1, France. Melting points were measured in evacuated capillaries on a Kofler Bristoline melting point apparatus and were not corrected.

2.2. Synthesis of complex 1

A solution of Cu(**2-TTA**)$_2$ (0.1842 g, 0.364 mmol) in $CHCl_3$/MeOH (15 mL, v/v, 2:1) was added to a solution of **4-stpy** (0.0600 g, 0.182 mmol) in $CHCl_3$ (5 mL) and the reaction mixture was stirred at room temperature (r.t.) for 15 min. The solution was left to stand at r.t. for 3 days; dark green blocks suitable for single crystal X-ray analysis were deposited. After filtration, the crystals were washed with ethanol and dried at 60°C in an oven overnight. Yield: 192.3 mg (0.088 mmol, 48.6 %). M.p.: 198-200 ºC. Anal. Calcd for $C_{88}H_{52}Cu_3F_{18}N_6O_{12}S_8$: C, 48.56; H, 2.50; N, 3.86; S, 11.78. Found: C, 48.21; H, 2.43; N, 3.66; S, 11.78. FT-IR (KBr, cm^{-1}): 3103(w), 3082(w) ν(C-H arom); 2958 (w), 2952(w), 2854(w) ν(C-H aliph); 1614(vs); 1539 (vs) 1499(s) 1412 (vs) ν(C⋯O), ν(C⋯C) and/or ν(C⋯N); 1311 (vs), 1299 (vs), 1188 (vs) $\nu(CF_3)$; 784 (s), 719 (s) δ(C-H) (SC_4H_3). UV-Vis [λ_{max},nm (log ε)] CH_2Cl_2: 704 (2.00); 343 (5.79), 293 (5.62).

2.3. Crystal structure determination

X-ray data for compound **1** were collected at 150(2) K on an APEXII, Bruker-AXS diffractometer, equipped with a bidimensional CCD detector using graphite-monochromated Mo-Kα (λ = 0.71073 Å) radiation. The structure was solved by direct methods using the *SIR97* program, [39], and then refined with full-matrix least-square methods based on F^2 (*SHELXL-97*) [40]. The contribution of the disordered solvents to the structure factors was calculated by the PLATON SQUEEZE procedure [41] and then taken into account in the final SHELXL-2014 least-square refinement [42]. The thiophene fragment in one of the **2-TTA** ligand coordinated to Cu(2) was modelled using two positions per carbon and sulfur atoms with occupancy factors of 0.70:0.30. The -CF_3 groups of the second **2-TTA** ligand bonded to Cu(2) exhibits rotational disorder with occupancies manually set to 50:50 ratio. All non-hydrogen atoms were refined with anisotropic atomic displacement parameters. H atoms were finally included in their calculated positions. A final refinement on F^2 with 10764 unique intensities and

606 parameters converged at $\omega R(F^2)$ = 0.1291 ($R(F)$ = 0.0502) for 8436 observed reflections with $I > 2\sigma(I)$. A summary of the details about crystal data collection parameters and refinement are documented in **Table 1**. Additional crystallographic details are in the CIF files. ORTEP views are generated using OLEX2. [43].

Table 1. Crystallographic data, details of data collection and structure refinement parameters for complex **1**.

Empirical Formula	$C_{88}\ H_{54}\ Cu_3\ F_{18}\ N_6\ O_{12}\ S_8$
Formula mass, g mol^{-1}	2176.47
Collection T, K	150(2)
Crystal system	Triclinic
Space group	P-1
a (Å)	13.3721(4)
b (Å)	13.8665(5)
c (Å)	14.9743(5)
α (°)	77.340(2)
β (°)	70.6350(10)
γ (°)	64.6380(10)
V (Å^3)	2357.33(14)
Z	1
D_{calcd} (g cm^{-3})	1.533
Crystal size (mm)	0.57 x 0.29 x 0.24
F(000)	1097
abs coeff (mm^{-1})	0.945
θ range (°)	2.95 to 27.53
range h,k,l	-17/14,-18/18,-19/18
No. total refl.	20984
No. unique refl.	10764
Comp. to θ_{max} (%)	99.2
Max/min transmission	0.797/0.707
Data/Restraints/Parameters	10764/0/606
Final R	R_1 =0.0502
[$I>2\sigma(I)$]	wR_2 =0.1291
R indices (all data)	R_1 =0.0656,wR_2 =0.1394
Goodness of fit / F^2	1.040
Largest diff. Peak/hole (eÅ^{-3})	1.084/-0.841

3. Results and Discussion

3.1. Syntheses and characterization

The new copper(II) complex **1**, [Cu_3(**2-TTA**)$_6$(**4-stpy**)$_2$], was obtained by mixing **4-stpy** ligand with Cu(**2-TTA**)$_2$ in a $CHCl_3$/MeOH solution (**Scheme 2)**. After 3 days, dark green blocks suitable for X-ray structure deposited. Complex **1** was obtained in moderate yield (~50%). The isolated product was separated as green air-stable solid and was fully characterized by elemental analysis, spectrometric (UV–Vis and IR), electrochemistry and magnetic measurements. This compound is insoluble in solvents

such as ethanol and methanol, however it is soluble in solvents like dichloromethane, DMF and DMSO.

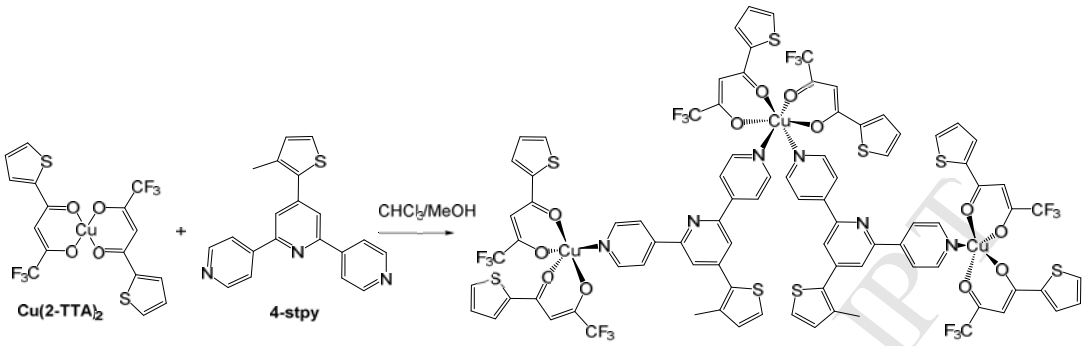

Scheme 2. Synthesis of complex **1**.

The solid-state FT-IR spectrum (**Fig. S1**), shows two weak bands at 3103 and 3082 cm^{-1} attributed to the unsaturated *ν*C-H stretching vibration mode of the aromatics rings. Three other weak bands at 2958, 2952 and 2854 cm^{-1} are due to the *ν*C-H stretching vibration of the aliphatic moiety (-CH_3). Additionally, the spectrum exhibits a series of bands between 1614 and 1412 cm^{-1} indicating the presence of the *ν*(C⋯O), *ν*(C⋯C) and *ν*(C⋯N) bonds.[44]. Besides, a series of three strong bands in the 1300-1100 cm^{-1}, were assigned to the stretching vibration mode of the C-F bonds in the -CF_3 groups [45,46]. The thienyl (Th) moiety was confirmed due to the presence of strong bands at 784 and 719 cm^{-1} and attributed to the out of plane bending vibration mode of the C-H groups present in this moiety [47,48]. This information is consistent with the crystal structure determined by X-ray diffraction (see below).

3.2. Structural Description of complex 1

Complex **1** crystallized in the triclinic centrosymmetric *P-1* space group with a half unit in the unit cell; a crystallographic inversion center lies in the Cu(1) atom, with a 50% occupancy. A perspective view of compound **1** with the atom labelling scheme is shown in **Fig. 1**, while selected bond distances and angles are listed in **Table 2**. Intermolecular hydrogen bonds are listed in **Table S1**. Aromatic interactions are described in **Tables S2** and **S3**.

The single crystal analysis revealed that the asymmetric unit contains two copper atoms (Cu(1) and Cu(2)) connected by the nitrogenous base (**4-stpy**) that acts as a bridge, linking the two metal centers to form a trinuclear complex and exhibiting a chain

structure between the axes ***a*** and ***c.*** **(Fig. 1).** Cu(1) is coordinated by only one **2-TTA** ligand, instead of Cu(2), that has two **2-TTA** coordinated ligands.

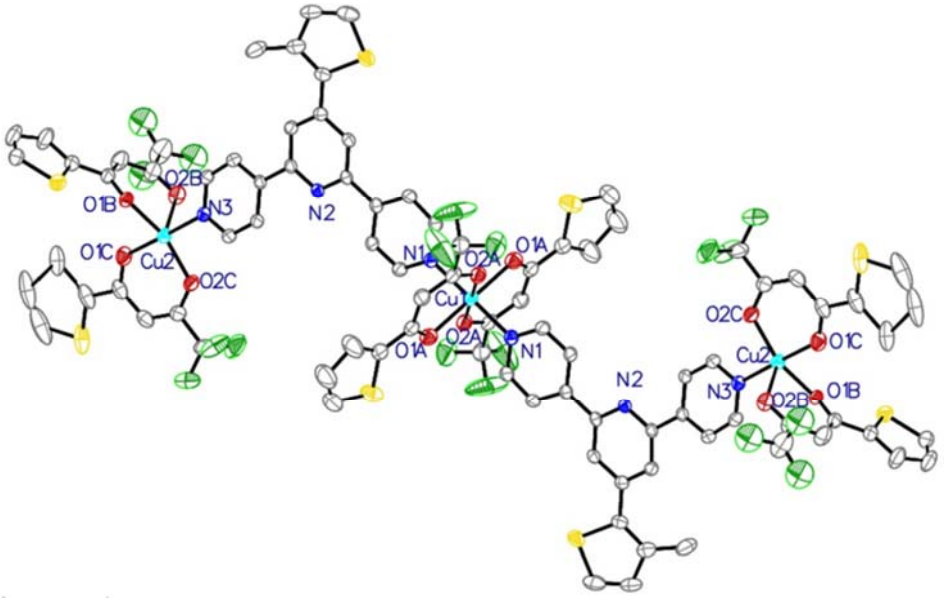

Fig. 1. Molecular structure of **1** with atom numbering scheme. The thermal ellipsoids are drawn at the 50% probability level and the hydrogen atoms are omitted for clarity.

In this structure, Cu(1) and Cu(2) centers adopt different geometries. The central copper atom Cu(1) is hexa-coordinated in an octahedral environment, showing the usual Jahn-Teller distortion [49,50], with the apical Cu(1)-O(1A) bond being 11% longer than the two remaining in the equatorial plane (**Fig. 2a, Table 2**). The equatorial sites are occupied by O2A, O2A', N1 and N1'. On the other hand, the Cu(2), is pentacoordinated in a slightly distorted square pyramidal geometry defined by N(3), O(1B), O(1C) and O(2C) atoms occupying the basal plane, and O(2B) in the apical position (**Fig. 2b**). To be noticed, the apical position distance for Cu(1) is longer than the one for Cu(2) (2.249(2) Å *vs.* 2.156(2)Å). (**Table 2**).

Cu(1) atom is immersed in its equatorial plane, while Cu(2) atom is raised 0.2346(15)Å above the square basal plane, presenting a distortion of the square pyramidal geometry (**Fig. 2**). Using the Addison's model [51], we found that the degree of trigonality for this five-coordinate metal center is: $\tau = 0.37$, which indicates that the geometry for Cu(2) is close to being square-based pyramidal, rather than trigonal bipyramidal.

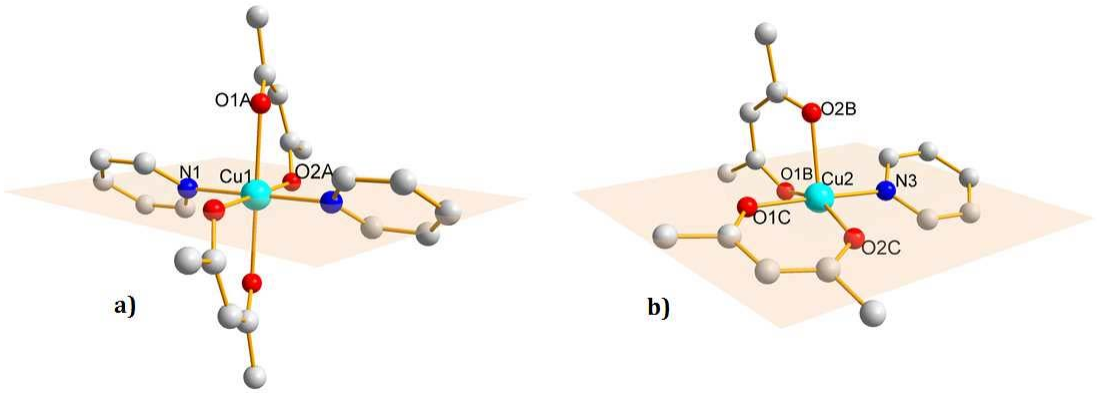

Fig. 2. Details of the coordination geometries for copper atoms: **a)** Octahedral Cu(1) and **b)** Slightly distorted square pyramidal Cu(2).

There are also some differences in the manner that ligands approach the metallic cation. In particular, the "slanting angle" or "inclination" that is, the way the **2-TTA** ligand approaches the metal centre. This one can be measured by the dihedral angle between two planes: the first one subtended by the O–Cu–O mean plane and the second one formed by the **2-TTA** ligand mean plane (**Fig. 3**, blue and green planes, respectively). The corresponding values for the “slanting angle” are: 21.08(15)° for the Cu(1) moiety (**Fig. 3a**), and 22.52(14)° and 5.99(18)° for the Cu(2) moiety (**Fig. 3 b**).

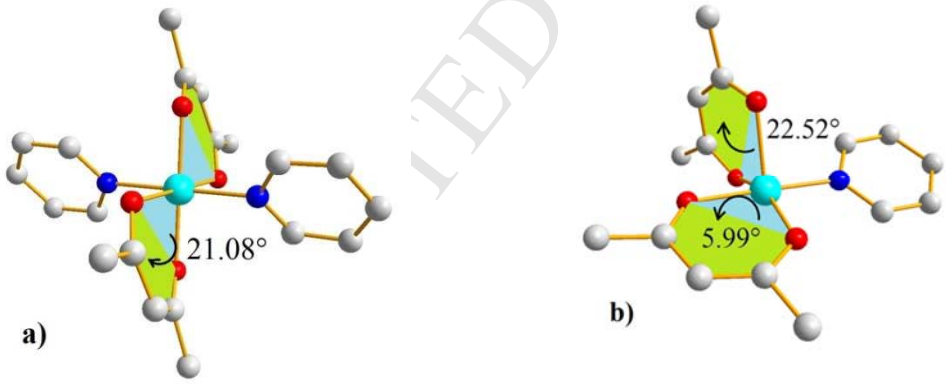

Fig. 3. Details of “slanting angle” for **a)** Octahedral Cu(1) and **b)** square pyramidal Cu(2).

This could be also the reason why the **4-stpy** ligand is not completely flat. As we can see, the two external pyridine rings of the terpyidine (that contains N1 and N3) generate mean planes that are twisted with respect to the central pyridine central ring which contains N2 atom. The mean planes between pyridine rings containing the N1/N2 atoms present a twist angle of 4.35(11)°, whereas that between pyridine rings containing the N2/N3 atoms, present a twist angle of 12.30(11)°. The most twisted pyridine ring is the

one containing N3 coordinated to the Cu(2) atom. The thienyl (Th) ring of **4-stpy** is twisted 16.92(13)° out of the plane with respect to the pyridine central ring to which it is attached.

Concerning the three types of **2-TTA** ligand, the C-O bonds adjacent to the Th substituent are slightly shorter compared to that of the -CF_3-substituted side (**Table 2**). The opposite trend is observed for the β-diketonato carbon backbone where the C-C(Th) bond is slightly longer than the C-C(-CF_3) bond. Both bonds exhibit double bond character, typical of β-diketonato ligands [52-54]. Due to this slight asymmetry in bond lengths, the associated bond angles are affected, with the O-C(-CF_3)-C angles ~5° larger than the O-C(Th)-C angles (**Table 2**). In one of the **2-TTA** ligand attached to Cu(2) , there is significant rotational disorder associated with the -CF_3 group, so C-F bond lengths vary significantly (1.252(10)- 1.496(10) Å). The C-F bond distances average 1.289 and 1.325 Å in the two others non disordered -CF_3 groups. On the other hand, the thienyl ring of the second **2-TTA** ligand linked to Cu(2) is disordered over two positions, a quite common observation for this unit [55,56]. However, the bond lengths and angles of the three different thienyl groups remain unexceptional [57].

Table 2. Selected bond distances (Å) and angles (°) for compound **1**

Bond distances			
Cu(1)—O(1A)	2.248(2)	Cu(2)—O(1B)	1.988(2)
Cu(1)—O(1A)^{i}	2.248(2)	Cu(2)—O(2B)	2.155(2)
Cu(1)—O(2A)	2.004(2)	Cu(2)—O(1C)	1.942(2)
Cu(1)—O(2A)^{i}	2.004(2)	Cu(2)—O(2C)	1.918(2)
Cu(1)—N(1)	2.020(2)	Cu(2)—N(3)	2.003(2)
Cu(1)—N(1)^{i}	2.020(2)	O(1B)—C(1B)	1.267(3)
O(1A)—C(1A)	1.240(4)	O(2B)—C(3B)	1.243(4)
O(2A)—C(3A)	1.265(4)	O(1C)—C(1C)	1.265(4)
C(1A)—C(2A)	1.434(4)	O(2C)—C(3C)	1.272(4)
C(2A)—C(3A)	1.372(5)	C(1B)—C(2B)	1.403(4)
C(5A)—S(2)	1.712(3)	C(2B)—C(3B)	1.390(5)
C(8A)—S(2)	1.687(5)	C(1C)—C(2C)	1.415(5)
C(4A)—F(4A) averages	1.289	C(2C)—C(3C)	1.367(5)
C(4B)—F(4B) averages	1.353	C(5B)—S(3)	1.710(3)
C(4C)—F(4C) averages	1.320	C(8B)—S(3)	1.709(3)
		C(5C)—S(4) averages	1.6585
Angles			
O(1A) —Cu(1)— O(1A)^{i}	180.0	O(1B)—Cu(2)—O(2B)	88.15(9)
O(2A)^{i}—Cu(1)— O(1A)^{i}	86.77(9)	O(1B)—Cu(2)—N(3)	90.90(9)
O(2A)^{i}—Cu(1)— O(1A)	93.23(9)	O(1B)—Cu(2)—O(1C)	86.66(9)
O(2A) —Cu(1)— O(1A)^{i}	93.23(9)	O(2B)—Cu(2)—O(1C)	89.59(9)
O(2A) —Cu(1)— O(1A)	86.77(9)	O(1C)—Cu(2)—N(3)	176.98(10)

$O(2A)^{i}$—Cu(1)— O(2A)	180.0	O(1B)—Cu(2)—O(2C)	154.90(9)
$O(2A)^{i}$—Cu(1)— N(1)	89.71(9)	O(1C)—Cu(2)—O(2C)	91.56(9)
O(2A) —Cu(1)— $N(1)^{i}$	89.71(9)	O(2B)—Cu(2)—O(2C)	116.89(9)
$O(2A)^{i}$—Cu(1)— $N(1)^{i}$	90.29(10)	N(3)— Cu(2)—O(2C)	89.90(9)
O(2A) —Cu(1)— N(1)	90.29(10)	N(3)— Cu(2)—O(2B)	92.12(9)
$N(1)^{i}$ — Cu(1)—$O(1A)^{i}$	87.94(9)	O(1B)—C(1B)—C(2B)	125.2(3)
$N(1)^{i}$ — Cu(1)—O(1A)	92.06(9)	O(2B)—C(3B)—C(2B)	130.1(3)
N(1) — Cu(1)—O(1A)	87.94(9)	C(1B)—C(2B)—C(3B)	123.9(3)
N(1) — Cu(1)—$O(1A)^{i}$	92.06(9)	O(1C)—C(1C)—C(2C)	123.4(3)
$N(1)^{I}$ — Cu(1)—N(1)	180.00	O(2C)—C(3C)—C(2C)	128.9(3)
O(1A)—C(1A)—C(2A)	125.2(3)	C(1C)—C(2C)—C(3C)	122.4(3)
O(2A)—C(3A)—C(2A)	130.5(4)		
C(1A)—C(2A)—C(3A)	124.5(4)		

Symmetry codes:(i) 2-X,1-Y,-Z

Intramolecular and classical hydrogen bond interactions were not found in the structure. However, the interactions to generate the supramolecular architecture between chains are diverse. Due to the presence of -CF_3 groups, intermolecular hydrogen bonds are present (**Fig. S2**, **Table S1**). There are also aromatic interactions involving C-F···π bonds (**Fig. S3**, **Table S2)** and the classical π-π interaction between central rings of terpyridine ligands (**Fig. S4**, **Table S3**). This diversity of binding interactions gives stability to the packing mode. To understand the magnetic behaviour discussed later is important to mention that the distance Cu(1)···Cu(2) along the chain is 12.6687 (5) Å, while the shortest inter-chain distance, for Cu(2)···Cu(2), is 5.2266 (10) Å.

Finally, all factors mentioned above are the result of the local steric hindrance in each metal coordination environment. The significant structural differences between the copper centers generate a complex with a discrete structure. The arrangement of the voluminous **2-TTA** groups in the vicinity of Cu (2) prevents the possibility of a sixth coordination, in which a nitrogen of the **4-stpy** ligand could be coordinated, presumably explaining why an extended coordination polymer is not formed. This kind of coordination compounds, between a 4,2':6',4"-terpyridine derivatives and bis(β-diketonate) complexes, has not been observed previously; instead, many coordination polymers have been reported [18,19] discrete structures like that of complex **1** being very scarce [58,59].

3.3. UV/Vis Studies

The knowledge of the orbital nature is important because many physical properties depend on the energy differences between frontier orbitals (*i.e.* HOMO, LUMO, SOMO). The electronic absorption spectra of both ligand **4-stpy** and compound **1** were measured in CH_2Cl_2 solutions. The absorption spectra in the UV region for both compounds show structured bands below 425 nm. These absorption spectra are shown in **Fig. 4a**. For **4-stpy**, two well-defined bands are centered at 233 nm (log ε= 4.47) and 272 nm (log ε= 4.52), with a shoulder at 307 nm (log ε = 4.27). These absorption bands can be attributed to a π→π* transition of conjugate systems. [29]

By contrast, complex **1** shows two well-defined bands centered at 293 nm (log ε= 5.62) and 343 nm (log ε= 5.79). The absorption bands are red-shifted compared to the free ligand, due to the coordination to the Cu^{2+}. They can be attributed to a mixture to π→π* and intramolecular charge-transfer (ICT) transition.

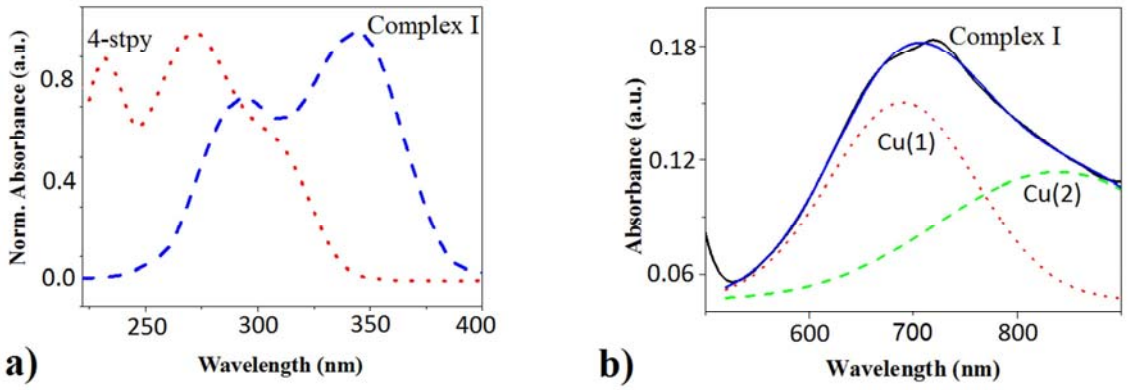

Fig. 4. Electronic absorption spectra in CH_2Cl_2 solutions : **a)** UV region, **4-stpy** (dotted red line) and complex **1** (dashed blue line). **b)** Visible region, complex **1** (black line) shows the deconvolution of the *d–d* transition band: for Cu(1) atom (red dotted line, octahedral environment) and Cu(2) atom (green dashed line, square pyramidal environment).

The Visible absorption spectrum shows a broad absorption in the range 500–900 nm (**Fig. 4b**). The broadness of the absorption band and its slighty asymmetrical shape suggest *d-d* transitions of copper(II) complexes undergoing distortions in their geometries.[60]

Since this molecular system involves three copper atoms, with two different geometric environments, one octahedral and two distorted square pyramidal, the spectrum in the

visible region (transition *d-d*) should present both absorption maxima, as suggested from **Scheme 3**.

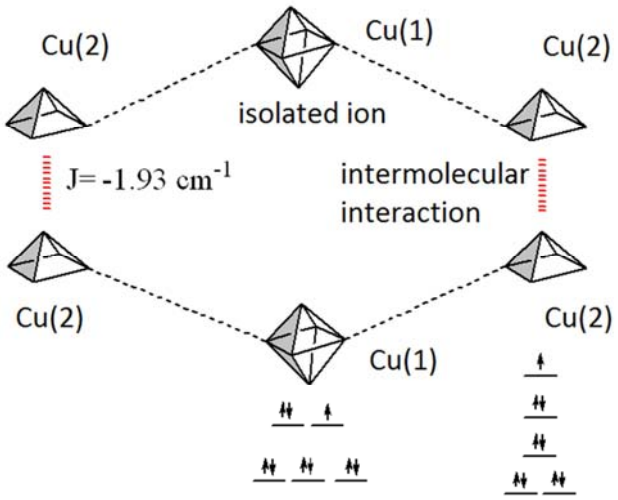

Scheme 3. Two environment (square pyramidal and octahedral) for copper atoms in the trinuclear complex **1** and their magnetic interaction.

A qualitative analysis of the UV spectrum in the visible region (**Fig. 4b**) allows a deconvolution of the absorption band of complex **1**. Two maxima are seen: one of them, *ca.* 838 nm, is assigned to a *d–d* transition for the Cu(2) atom with square-pyramidal geometry [61] and the other, corresponding to a high energy shift of the bands below 700 nm, is assigned to a *d–d* transition for the Cu(1) atom with octahedral geometry. [62]

3.4. TGA/ DSC

To investigate the thermal stability of compound **1**, thermogravimetric analyses were performed in the 30-600 °C range on a solid sample consisting of numerous single crystals at a heating rate of 10°C min^{-1} under a nitrogen atmosphere. **Fig. 5** shows the TG/DTG/DSC curves for complex **1**. The thermogram presents two mass-loss stages. The first weight-loss process of ~ 5% occurs at 181.3 °C, associated with a small endothermic event displayed in the DSC curve. This is characteristic of the loss of adsorbed solvent molecules. The next endothermic peak, without a mass loss and centered at 200.50 °C is attributed to a melting event. This process is confirmed by direct observation in a melting-point microscope instrument. By comparing the TG and DSC curves, it is evident that the thermal decomposition begins at a higher temperature than the melting point of the compound, and so it occurs in the liquid phase.

The DTG curve shows that the main event occurs with a peak centered at 293.42 °C with a total weight loss of ~56% (Calc. 61%), that involves a combination of exothermic peaks displayed in the DSC curve. This process can be attributed to the decomposition of organic groups, mainly the **2-TTA** groups, accompanied by a continuous decomposition processes of **4-stpy**, which continues until our limiting temperature of 600 °C.

The thermal properties of coordination complexes are determined by the chemical properties of the metal center and coordinated ligands. In this case, we can see that the decomposition temperature of complex **1** is lowered in relation to the precursors, Cu(**2-TTA**)$_2$ and **4-stpy** (315 °C and 363°C, respectively) [29,36].

The difference on the decomposition temperature between these compounds can be attributed to electronic effects, since the coordination of **4-stpy** can make that the Cu-**2-TTA** bond in complex **1** becomes weaker and less stable; as a consequence, the **2-TTA** ligand is liberated at a lower temperature than expected.

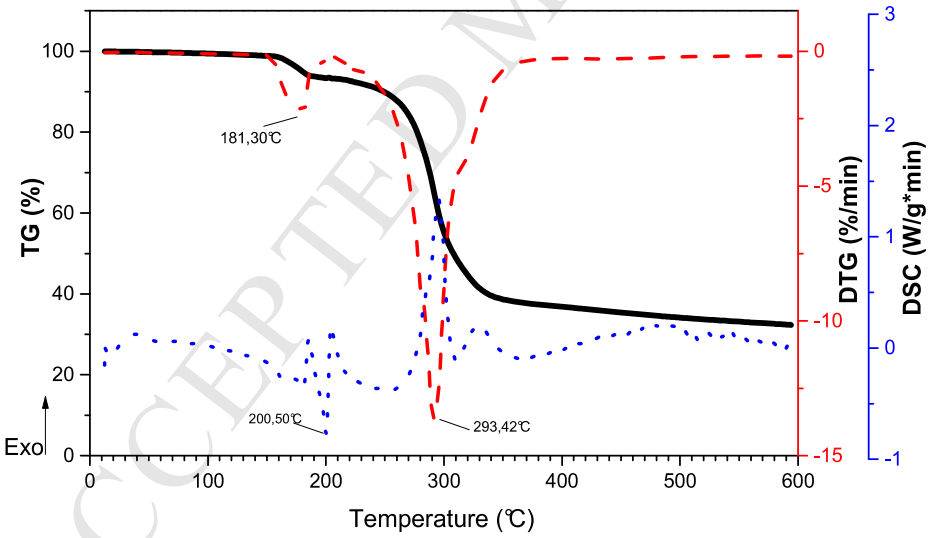

Fig. 5. TGA and DSC curves for complex **1**

3.5. Magnetism

Fig.6 shows the magnetic behavior of compound **1**. From the inverse molar susceptibility vs temperature (insert, **Fig.6**), a magnetic moment of 1.76 μ_B per copper(II) center is obtained, quite close to the expected value for one unpaired electron

having a spin contribution S=½ (μ_{eff} = 1.74 μ_B). This is in agreement with the general behavior of a simple paramagnetic system.

The main graph, **Fig.6**, shows the temperature dependence of the product $\chi_M \cdot T$. A quite constant behavior is observed between room temperature and 60 K, with a value which corresponds to the effective moment of 1.76 μ_B. At lower temperature there is a strong decrease, indicating weak antiferromagnetic interactions. A possible explanation for this decrease could be a single ion anisotropy of the copper atom. However, since we are in presence of a trinuclear copper complex, magnetic interactions probably exist between the paramagnetic centers.

Based on the structural data, an intermolecular interaction between Cu(2) centers is postulated (distance of 5,226 Å), while Cu(1) remains isolated (its distance to other Cu(1) center is larger than 12 Å). Since this system obeys to a 2:1/ Cu(2):Cu(1) proportion, as shown in **Scheme 3**, we have fitted the experimental data to a combination of dimers and monomers in the same ratio, finding a weak antiferromagnetic interaction (see **Equation 1**). [63]

$$\chi_M = \frac{2N\beta^2}{k} \cdot \frac{g^2}{(T+\theta_d)} \cdot \frac{1}{[3+e^{(-\frac{J}{kT})}]} \cdot (1-\rho) + \rho \cdot \frac{g^2}{(T+\theta_{mon})} \cdot \frac{N\beta^2}{2k}$$ **Equation 1**

where all symbols have their usual meaning (*N, k, β, θ_x* and *g* are, respectively, the Avogadro's number, the Boltzmann's constant, the Bohr magneton, temperature correction factors and the Landé g-factor) whereas *ρ* is the molar fraction of uncoupled monomer species.

Using the above relations, the best fit to the experimental data, as shown in **Fig. 6**, yielded *g* = 2.16 (in agreement with the value obtained from the EPR analysis), *J* = -1.93 cm^{-1} and ρ= 30% (R= $1.05 \cdot 10^{-6}$, where R is defined as R= $\Sigma[(\chi_M)_{obs}-(\chi_M)_{cal}]^2/\Sigma[(\chi_M)_{obs}]^2$).

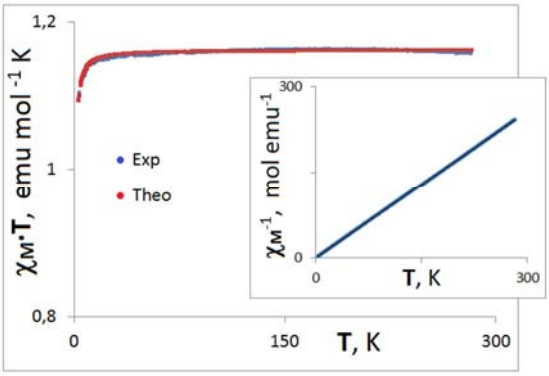

Fig. 6. Temperature dependence of $\chi_M T$ for complex **1**. Insert, temperature dependence of χ_M^{-1}.

The EPR data are in agreement with the results obtained from susceptibility measurements. The X-Band room temperature EPR spectrum measured on powders is represented on **Fig. 7**. The broad signal covers more than 500 G with a main feature at g = 2.11 corresponding to the equatorial contributions and a shoulder at g = 2.25 corresponding to the axial contribution. This spectrum is typical of Cu(II) centers with an average g value equal to 2.16.

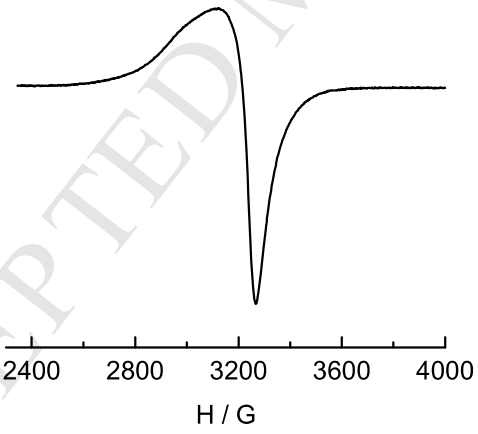

Fig. 7. Room temperature X-band EPR spectrum on powders for complex **1**.

3.6. Cyclic Voltammetry

The electrochemical behavior of the **4-stpy** ligand and complex **1** were investigated by means of cyclic voltammetry (CV) technique. First, CV experiments were carried out in the anodic range potential of -0.5 to 2.0 V *vs.* Fc/Fc^+. In this range, neither the **4-stpy** ligand nor complex **1** exhibit any oxidation process. On the contrary, the previously reported compound Cu(**2-TTA**)$_2$ shows a process which occurs near 1.95 V attributed to

the mono-oxidation of the thienyl rings; [64] this process is not observed in our case. We believe that, due to the presence of the terpyridine moiety in the complex, the stability of this compound is enhanced by the increased conjugation in the system, hindering any oxidation process attributable to the thienyl rings of the **2-TTA** fragment. Moreover, the presence of strong electron withdrawing -CF_3 groups renders very difficult the oxidation of the thienyl unit present in the terpyridine moiety.

On the other hand, CV experiments were carried out in the cathodic potential range of 0 to -2.6 V for the **4-stpy** ligand and in the range of -0.5 to -3.0 V for complex **1**. In the case of **4-stpy**, a reduction peak was observed at -2.40 V (**Fig. 8**). For complex **1**, three processes were observed at -1.34, -1.90 and -2.50 V *vs.* Fc/Fc^+ (**Fig. 8**). The first two redox events could be attributed to the $Cu^{2+}|Cu^+$ and $Cu^+|Cu^o$ couples, respectively [64]. Due to the large distance between the copper atoms (see section 3.2), we can assume that the reduction of the three metal ions are observed as one redox process for each oxidation state ($Cu^{2+}|Cu^+$ and $Cu^+|Cu^o$), indicating that the three copper centers are electrochemically equivalent.

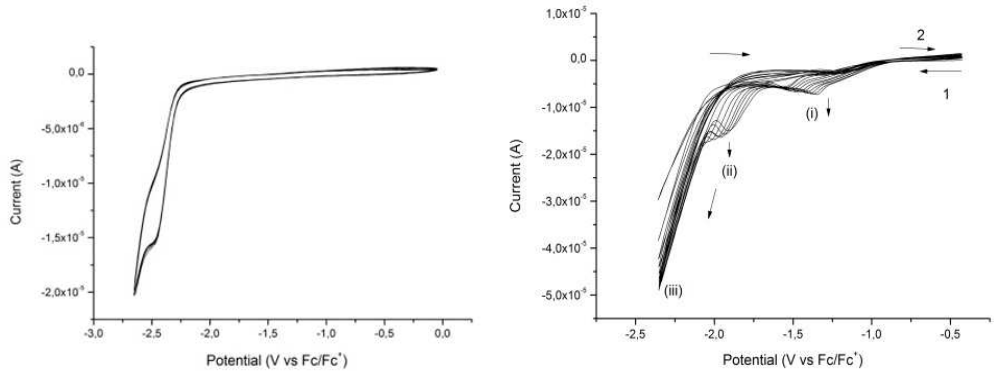

Fig. 8. Cyclic voltammograms of **4-stpy** (left) and complex **1** (right) recorded in acetonitrile containing 0.1 M *n*-$Bu_4N^+PF_6^-$ as supporting electrolyte, at Pt electrode, 20 °C, v = 0.1 V s^{-1}. Potentials are refered to Fc/Fc^+ couple.

Compared to the CV of the free **4-stpy** (**Fig. 8**), the third process, the most negative one, was attributed to the reduction of the **4-stpy** ligand moiety. In addition, we observed that for each cycle of the voltammogram, the current response increases and the potential is shifted toward higher potential ranges. This behavior should correspond to a modification of the electrode surface, as confirmed at the end of each experiment, where metallic copper was observed on the surface of the electrode.

4. Conclusions

Using an appropriate ligand, such as bis(β-diketonate), **2-TTA**, it is possible to adjust the chemical reactivity of the metal center, changing their electronic density to allow the fifth and sixth coordination of **4-stpy** ligand in the Cu(II) center. In contrast to related structures in the literature, this is one of the few examples of the bridging behavior of divergent 4,2':6',4"- terpyridine ligand, which gives rise to discrete molecular structures. We attribute the formation of the unexpected trinuclear complex mainly to a size tuning of the substituent groups in the bis(β-diketonate) and to the steric effect caused by the slanting angle of **2-TTA** groups, becoming less prone toward polymeric structures. The magnetic behavior is explained by a single model combining monomeric Cu(1) and dimeric Cu(2) species, in a ratio 2:1/Cu(2):Cu(1), resulting in a weak antiferromagnetic interaction (J= -1.93 cm^{-1}). Although this is an interesting study with its own challenges, there are still basic questions to answer about the influence of other metallic centers (for example, Zn(II), Ni(II) and Co(II), having different ionic radii, hardness, total magnetic spin, etc.) on the structural conformation and physical properties of these systems; in particular, coordination polymers against discrete molecules.

Acknowledgments

We gratefully acknowledge Dr. O. Cador (Rennes) for recording the EPR spectrum and helpful discussion of the magnetism. This research was performed as part of the Chilean-French International Associated Laboratory for ‘’Inorganic Functional Materials’’ (LIA-MIF-CNRS N°836). Financial supports FONDECYT (Chile), grant no: 1130433 (Y.M) and 1140903 (C.M.), the CNRS and the Université de Rennes-1 are gratefully acknowledged. Thanks to CONICYT (Chile) for support of graduate fellowships N°: 21120148 (D.T) and N°21120098 (G.A). Thanks to UNAB DI-773-15/R.

Appendix A. Supplementary material

CCDC 1529946 contains the supplementary crystallographic data for this paper. These data can be obtained free of charge from the Cambridge Crystallographic Data Centre via www.ccdc.cam.as.uk/data_request/cif.

References

[1] J.S. Miller, Inorg. Chem. 39 (2000) 4392-4408.

[2] R. Baggio, D. Contreras, Y. Moreno, R. Arrue, I.E. Paulus, O. Peña, J.-Y. Pivan, J. Coord. Chem 65 (2012) 2319-2331.
[3] M. Wałęsa-Chorab, A.R. Stefankiewicz, A. Gorczyński, M. Kubicki, J. Kłak, M.J. Korabik, V. Patroniak, Polyhedron 30 (2011) 233-240.
[4] D.A. Souza, A.S. Florencio, S. Soriano, R. Calvo, R.P. Sartoris, J. Walkimar de M. Carneiro, C. Sangregorio, M.A. Novak, M.G.F. Vaz, Dalton Trans. (2009) 6816-6824.
[5] L. Li, Y.Z. Zhang, C. Yang, E. Liu, J.A. Golen, G. Zhang, Polyhedron 105 (2016) 115-122.
[6] A.N. Kharat, A. Bakhoda, T. Hajiashrafi, J. Mol. Catal. A: Chemical 333 (2010) 94-99.
[7] J.-N. Li, Synth. React. Inorg. Met. Org. NanoMet. Chem. 43 (2013) 832-837.
[8] S. Roy, S. Saha, R. Majumdar, R.R. Dighe, A.R. Chakravarty, Polyhedron 29 (2010) 3251-3256.
[9] S. Wang, W. Chu, Y. Wang, S. Liu, J. Zhang, S. Li, H. Wei, G. Zhou, X. Qin, Appl. Organometal. Chem. 27 (2013) 373-379.
[10 G.J. Kharadi, Spectrochim. Acta Part A: Molecular and Biomolecular Spectroscopy 117 (2014) 662-668.
[11] D.A. Souza, Y. Moreno, E.A. Ponzio, J.A.L.C. Resende, A.K. Jordão, A.C. Cunha, V.F. Ferreira, M.A. Novak, M.G.F. Vaz, Inorg. Chim. Acta 370 (2011) 469-473.
[12] Z. Yin, Y.-L. Zhou, M.-H. Zeng, M. Kurmoo, Dalton Trans. 44 (2015) 5258-5275.
[13] A.Y. Robin, K.M. Fromm, Coord. Chem. Rev. 250 (2006) 2127-2157.
[14] J. Bai, H.-L. Zhou, P.-Q. Liao, W.-X. Zhang, X.-M. Chen, CrystEngComm 17 (2015) 4462-4468.
[15] J. Wang, G.S. Hanan, Synlett 8 (2005) 1251-1254.
[16] G.W.V. Cave, C.L. Raston, J. Chem. Soc., Perkin Trans. 1 (2001) 3258-3264.
[17] A. Winter, A.M.J. van den Berg, R. Hoogenboom, G. Kickelbick, U.S. Schubert, Synthesis (2007) 0642-0642.
[18] C.E. Housecroft, CrystEngComm 17 (2015) 7461-7468.
[19] C.E. Housecroft, Dalton Trans. 43 (2014) 6594-6604.
[20] A. Winter, M.D. Hager, G.R. Newkome, U.S. Schubert, Adv. Mater 23 (2011) 5728-5748.
[21] Z. Yin, S. Zhang, S. Zheng, J.A. Golen, A.L. Rheingold, G. Zhang, Polyhedron 101 (2015) 139-145.
[22] Y.M. Klein, A. Prescimone, E.C. Constable, C.E. Housecroft, Polyhedron Part A 103 (2016) 58-65.
[23] T.-T. Li, Y. Zheng, Q.-Y. Chen, S.-R. Zheng, J. Coord. Chem. 69 (2016) 966-975.
[24] J. Yoshida, S.-i. Nishikiori, R. Kuroda, Chem. Eur. J. 14 (2008) 10570-10578.
[25] J. Yoshida, S.-i. Nishikiori, H. Yuge, J. Coord. Chem. 66 (2013) 2191-2200.
[26] J. Granifo, R. Gaviño, E. Freire, R. Baggio, J. Mol. Struct. 1006 (2011) 684-691.
[27] J. Granifo, D. Toledo, M.T. Garland, R. Baggio, J. Fluorine Chem. 131 (2010) 510-516.
[28] J. Yoshida, S.-i. Nishikiori, R. Kuroda, Chem. Lett. 36 (2007) 678-679.
[29] D. Toledo, R. Baggio, E. Freire, A. Vega, N. Pizarro, Y. Moreno, J. Mol. Struct. 1102 (2015) 18-24.
[30] J. Roncali, Chem. Rev. 92 (1992) 711-738.
[31] J. Roncali, J. Mater. Chem. 9 (1999) 1875-1893.

[32] B.J. Holliday, T.B. Stanford, T.M. Swager, Chem. Mater. 18 (2006) 5649-5651.
[33] K.A. Williams, A.J. Boydston, C.W. Bielawski, Chem. Soc. Rev. 36 (2007) 729-744.
[34] M.O. Wolf, Adv. Mater. 13 (2001) 545-553.
[35] T.M.S.R.P. Kingsborough, Adv. Mater. 10 (1998) 1100-1104.
[36] Z. Chen, Y. Wu, F. Huang, D. Gu, F. Gan, Spectrochim. Acta Part A: Molecular and Biomolecular Spectroscopy 66 (2007) 1024-1029.
[37] W.L.F. Armarego, C.L.L. Chai, Purification of Laboratory 776 Chemicals, Fifth ed., Butterworth-Heinemann, Elsevier Inc., Amsterdam, The Netherlands, 2003.
[38] N.G. Connelly, W.E. Geiger, Chem. Rev. 96 (1996) 877-910.
[39] A. Altomare, M.C. Burla, M. Camalli, G.L. Cascarano, C. Giacovazzo, A. Guagliardi, A.G.G. Moliterni, G. Polidori, R. Spagna, J. Appl. Crystallogr. 32 (1999) 115-119.
[40] G.M. Sheldrick, Acta Crystallogr. Sect. A 64 (2008) 112-122.
[41] A.L. Spek, Acta Crystallogr. Sect. C 71 (2015) 9-18.
[42] G.M. Sheldrick, Acta Crystallogr. Sect. C 71 (2015) 3-8.
[43] O.V. Dolomanov, L.J. Bourhis, R.J. Gildea, J.A.K. Howard, H. Puschmann, J. Appl. Crystallogr. 42 (2009) 339-341.
[44] K. Nakamoto, Infrared and Raman Spectra of Inorganic and Coordination Compounds, John Wiley & Sons, Inc., 2008, DOI: 10.1002/9780470405888.ch1, pp. 1-273.
[45] R.L. Redington, K.C. Lin, Spectrochim. Acta Part A: Molecular Spectroscopy, 27 (1971) 2445-2460.
[46] S.P. Gejji, K. Hermansson, J. Lindgren, J. Phys. Chem. 97 (1993) 3712-3715.
[47] J.J. Peron, P. Saumagne, J.M. Lebas, Spectrochim. Acta Part A: Molecular Spectroscopy, 26 (1970) 1651-1666.
[48] P. Molina, A. Arques, I. Cartagena, in Comprehensive Heterocyclic Chemistry III, eds. C.A. Ramsden, E.F.V. Scriven, R.J.K. Taylor, Elsevier, Oxford, 2008, DOI: http://dx.doi.org/10.1016/B978-008044992-0.00309-6, pp. 625-739.
[49] M. Gerloch, Inorg. Chem. 20 (1981) 638-640.
[50] I. Bertini, D. Gatteschi, A. Scozzafava, Inorg. Chem. 16 (1977) 1973-1976.
[51] A.W. Addison, T.N. Rao, J. Reedijk, J. van Rijn, G.C. Verschoor, J. Chem. Soc., Dalton Trans. (1984) 1349-1356.
[52] A. Kuhn, S. Tischlik, K. H. Hopmann, M. Landman, P. H. van Rooyen, J. Conradie, Inorg. Chim. Acta 453 (2016) 345-356.
[53] S. Layek, S. Kumari Anuradha, B. Agrahari, R. Ganguly, D. D. Pathak, Inorg. Chim. Acta 453 (2016) 735-741.
[54] L.A.M. Baxter, A.J. Blake, R.O. Gould, G.A. Heath, T.A. Stephenson, Acta Crystallogr. Sect. C 49 (1993) 1311-1315.
[55] S. J. Howell, C. S. Day, R. E. Noftle, Inorg. Chim. Acta 358 (2005) 3711-3723.
[56] J. Oyarce, L. Hernández, G. Ahumada, J. P. Soto, M. A. del Valle, V. Dorcet, D. Carrillo, J.-R. Hamon, C. Manzur, Polyhedron 123 (2017) 277-284.
[57] F. H. Allen, O. Kennard, D. G. Watson, L. Brammer, A. G. Orpen and R. Taylor, J. Chem. Soc., Perkin Trans. 2 (1987) S1-S19.
[58] J. Granifo, R. Gaviño, E. Freire, R. Baggio, Acta Crystallogr. Sect. C 68 (2012) m269-m274.
[59] J. Granifo, R. Gaviño, E. Freire, R. Baggio, J. Mol. Struct., 1063 (2014) 102-108.
[60] D. Sutton, Electronic Spectra of Transition Metal Complexes, McGraw-Hill, New York, 1968.

[61] M. Zhou, L. Song, F. Niu, K. Shu, W. Chai, Acta Cryst. Sect C69 (2013), 463–466.
[62] E. Prenesti, P. G. Daniele, S. Berto, S. Tosso, Polyhedron 25 (2006) 2815‑2823.
[63] O.Kahn, Molecular Magnetism, Wiley-VCH, New York, 1993.
[64] M. A. Al-Anber, Am. J. Phys. Chem. 2 (2013) 1-7.

Highlights

- The molecular structure of an unusual trinuclear copper(II) complex, [Cu_3(**2-TTA**)$_6$(**4-stpy**)$_2$] (**1**), is presented.
- The trinuclear system has two different copper environments: octahedral and pyramidal.
- The contribution of each copper center to the UV-Vis spectrum has been identified and isolated.
- The intermolecular magnetic interaction between the pyramidal copper centers, has been identified.